International Conferences on Recent Advances in Geotechnical Earthquake Engineering and Soil Dynamics

1991 - Second International Conference on Recent Advances in Geotechnical Earthquake Engineering & Soil Dynamics

14 Mar 1991, 2:00 pm - 3:30 pm

Use of Rayleigh Modes in Interpretation of SASW Test

N. Gucunski
The University of Michigan, Ann Arbor, Michigan

R. D. Woods
The University of Michigan, Ann Arbor, Michigan

Proceedings: Second International Conference on Recent Advances in Geotechnical Earthquake Engineering and Soil Dynamics, March 11-15, 1991, St. Louis, Missouri, Paper No. 10.10

Use of Rayleigh Modes in Interpretation of SASW Test

N. Gucunski
Ph.D. Candidate, Department of Civil Engineering, The University of Michigan, Ann Arbor, Michigan

R.D. Woods
Professor, Department of Civil Engineering, The University of Michigan, Ann Arbor, Michigan

SYNOPSIS The Spectral-Analysis-of-Surface-Waves (SASW) method is a seismic method for measuring in situ elastic moduli of layered systems, like soils or pavements. The inversion process associated with SASW can be an ambiguous task in certain cases, because a field dispersion curve needs to be matched with an unknown path through a family of theoretically defined curves for an assumed profile. A study of the influence of soil stratification on participation of higher Rayleigh modes in surface wave propagation included the evaluation of theoretical dispersion curves, modal shapes and rates of energy transmission in the horizontal direction. Wave propagation due to oscillations of a circular plate on the surface of layered systems was modelled and the resulting "simulated" dispersion curves compared with theoretical ones. The results indicate that higher Rayleigh modes can dominate wave propagation for all but a narrow range of low frequencies for profiles where softer layers are trapped between stiffer layers. Potential ways of identification of such situations are discussed and improvements of the inversion process suggested.

INTRODUCTION

The shear modulus of soil is an essential parameter in design of dynamically loaded foundations, pavements, vibration barriers, and all other dynamically excited structures resting on soil. In most cases the produced shear strain level is so low, that behavior may be characterized as essentially linearly elastic.

The Spectral-analysis-of-surface-waves (SASW) method is a seismic method for measuring in situ elastic moduli of layered systems and has been developed during past ten years.The SASW method has advantages over borehole techniques because it is performed from the surface and it is a simple procedure with the prospect of being fully automatized. Comparison with crosshole test results by Hiltunen and Woods (1988), Nazarian at al. (1983), and Nazarian and Stokoe (1984 and 1986) confirmed the high level of accuracy of the SASW method in most of cases. Experience which the authors have gained during several SASW measurements is that in the case of irregular soil profiles (where a soft soil layer exists between hard soil layers) obtaining a unique solution may be an ambiguous task.

The ambiguity of uniqueness of a derived soil profile is attributed to a potential strong influence of waves of higher Rayleigh modes on the overall propagating pattern. The purpose of this paper is to explore analytically the influence of the soil layer properties and sequence on the participation of multiple Rayleigh modes and to provide guidelines for their identification and interpretation on the field.

DESCRIPTION OF THE SASW METHOD

The SASW method is based on the dispersive characteristic of surface waves in layered media, in this case Rayleigh waves. The dispersive characteristic of Rayleigh waves means that a group of surface waves of different frequencies propagates with different velocities. A general configuration of the SASW test is shown in Fig. 1. Propagating waves are detected by the receivers and recorded by the dynamic signal analyzer.

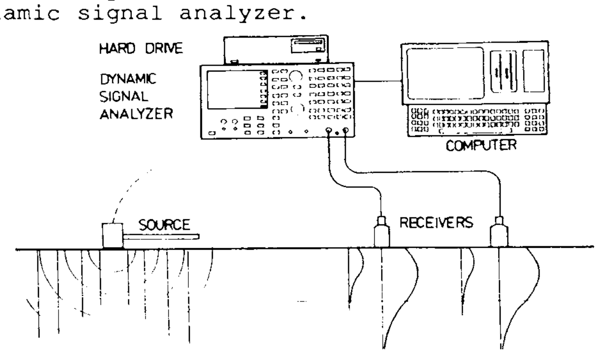

Fig. 1. General configuration of SASW test.

Transformation of recorded signals from the time to the frequency domain enables execution of several operations. Among these operations the phase of the cross power spectrum and the coherence are of the greatest importance. They contain information on frequency-phase velocity relations and quality of the recorded signal, respectively. The phase of the cross power spectrum, shown in Fig. 2a, represents a phase shift of a signal between two receivers as a function of frequency.

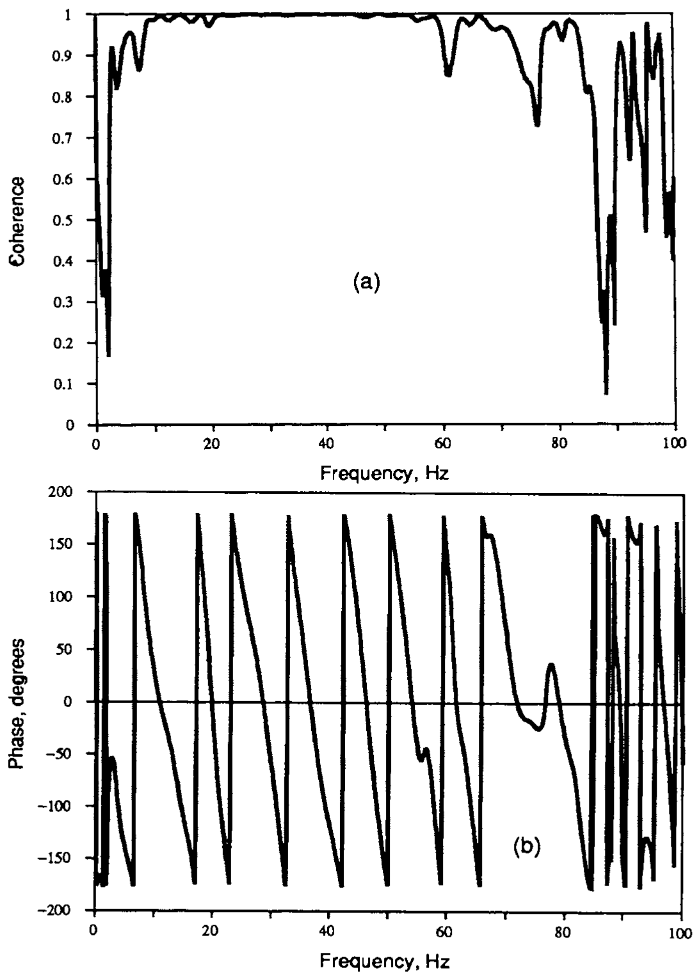

Fig. 2. A typical cross power spectrum (a) and the corresponding coherence (b).

From the cross power spectrum a phase velocity-wave length curve, the dispersion curve, can be plotted by use of a known receiver spacing. It is done in terms of equations (1) and (2),

$$V_{ph} = \frac{360xf}{\beta} \quad (1)$$

$$\lambda_{ph} = \frac{V_{ph}}{f} \quad (2)$$

where V_{ph} represents the phase velocity, x is the receiver spacing, f is frequency in Hz, ß the phase shift in degrees, and λ_{ph} the wave length.

The dispersion curve, like the one shown in Fig. 3, is a basis for the definition of a soil profile in terms of thicknesses of layers and corresponding shear wave velocity. The inversion process at the current stage consists of an iterative procedure in which a dispersion curve developed from a theoretical solution for an assumed profile is being matched with a field determined dispersion curve.

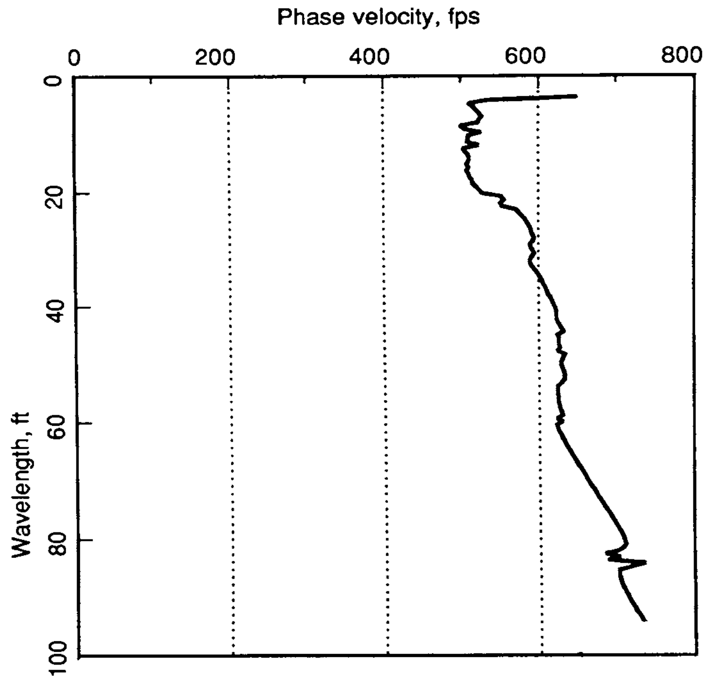

Fig. 3. Experimental dispersion curve.

PREVIOUS OBSERVATIONS OF THE INFLUENCE OF HIGHER RAYLEIGH MODES

Previous researchers have indicated a presence and, in some cases, a dominant effect of higher Rayleigh modes on the resultant surface wave propagation. Nazarian (1984) and Nazarian and Stokoe (1986) indicate modes of propagation with complex phase velocities in the case of a stiffer layer overlying a softer half-space. The solution in those cases was sought by assuming a multilayered plate resting on a layered half-space, as described by Ewing et al. (1957). As an illustration they provide an example of a two and a three-layered media where the dispersion curve consists of two branches as shown in Fig. 4. The flexural mode of vibration of a plate modified by the presence of the underlying half-space is presented by branch I, while the so called interfacial mode of vibration is presented by branch II. While the flexural mode has the dominant effect in the high frequency range, its influence vanishes for the low frequency range.

Sanchez-Salinero et al. (1987) in their analytical study of variables affecting surface wave testing of pavements indicate complications connected with the case of a stiff layer over a softer half-space. As Nazarian and Stokoe did they state the existence of a critical frequency below which there are no waves of Rayleigh type with a pure, real phase velocity. Also, in the case of a three-layer pavement, through the comparison of dispersion curves for plane Rayleigh waves and the one generated by a point load, they observed a shift from the first Rayleigh mode towards the higher Rayleigh modes as frequency increases. This is shown in Fig. 5. Based on those results they proposed a model for backcalculation of elastic properties, for the inversion process.

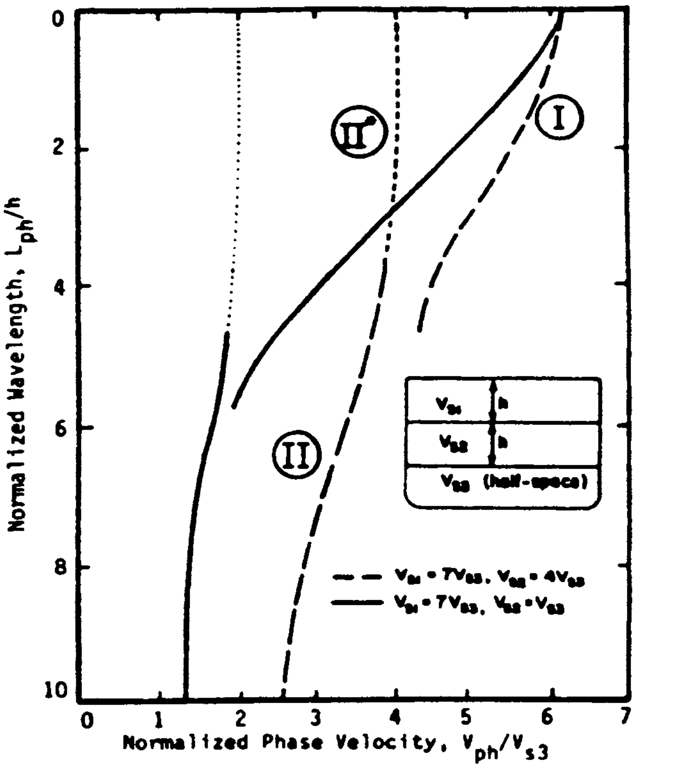

Fig. 4. Comparison of theoretical dispersion curves for two-layered and three-layered media (from Nazarian & Stokoe, 1986).

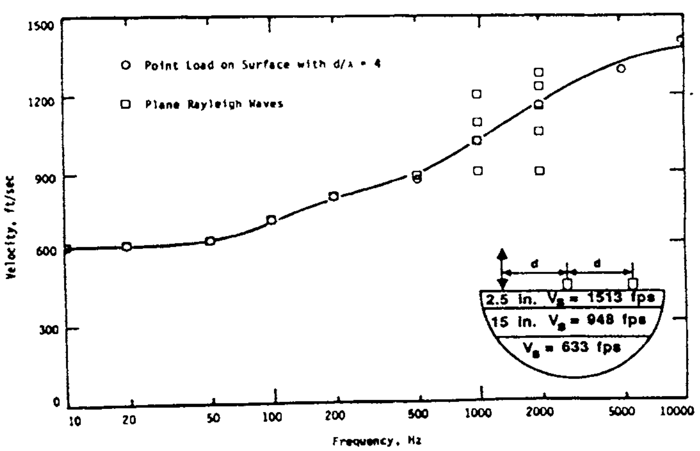

Fig. 5. Comparison of the dispersion curve produced by a point load on the surface of the pavement with the dispersion curves obtained assuming plane Rayleigh waves (from Sanchez-Salinero et al., 1987).

Douglas & Eller (1986) in their article on the Nondestructive pavement testing by wave propagation (NDPT/WP), the method as the SASW based on the generation of Rayleigh wave dispersion waves, acknowledge the problems involved in the selection of the family of curves from the dispersion field. The dispersion field, as shown in Fig. 6, is generated based on a field measurement with multiple receivers positioned radially away from the source.

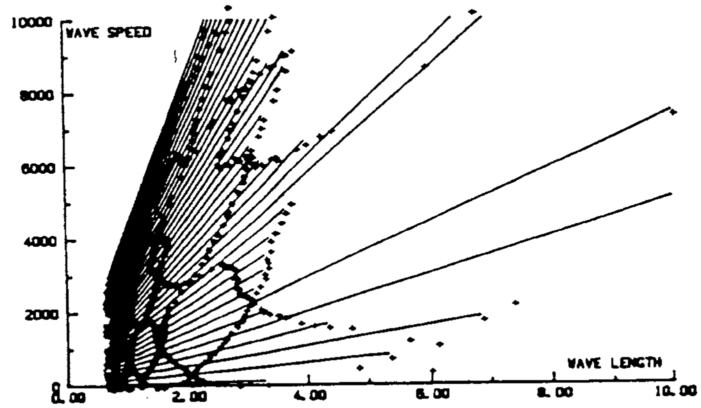

Fig. 6. Dispersion field before identification (from Douglas and Eller, 1986).

THEORETICAL BACKGROUND AND THE NUMERICAL ANALYSIS

The primary goal of the numerical analysis was to define and compare dispersion curves of multi-layered systems based on the plane wave approach and a dispersion curve generated from a numerical simulation of wave propagation along the surface of the same systems due to a circular impact source. To derive more complete understanding of the participation of higher Rayleigh modes in wave propagation caused by a circular impact source, the following additional elements were analyzed: the normalized rate of energy transmission, modal surface displacements, mode shapes, and the frequency-wave number domain surface displacements.

The mathematical formulation of wave propagation in layered systems was first presented by Thomson (1950) and Haskel (1953) and represents the so called transfer matrix approach. In this approach the transfer matrix of a layer, which relates displacements and stresses on the top and the bottom the layer in the frequency-wave number domain, is formed. Dispersion curves are obtained by forming a transfer matrix for the system in which the displacements and stresses at the surface and at the top of the half-space are related. Since Rayleigh waves can be interpreted as natural modes of vibrations of the layered system, they can be obtained by satisfying the conditions of zero surface loading and no incoming waves in the half-space.

An alternative approach to compute dispersion curves, which was used in this analysis, is by the stiffness matrix approach. The stiffness matrix of a soil layer, as an extension of the transfer matrix, was derived by Kausel and Roesset (1981), and in a slightly different form presented by Wolf and Obernhuber (1982) and Wolf (1985). The stiffness matrix relates forces at the top and the bottom of the layer with the displacements at the same in the frequency-wave number domain as shown in Table I for the in-plane motion. Variables involved in the table include: the frequency-wave number k, the thickness of a layer d, angular frequency ω, G^* the complex shear modulus, and V_p^* and V_s^* P- and S-wave complex velocity, respectively.

Table I. The stiffness matrix of a layer.

$$
\begin{Bmatrix} P_1 \\ R_1 \\ P_2 \\ R_2 \end{Bmatrix} = \frac{(1+t^2)\,kG^*}{D}
\begin{bmatrix}
\frac{1}{t}\cos ksd \sin ktd + s\sin ksd \cos ktd & \frac{3-t^2}{1+t^2}(1-\cos ksd \cos ktd) + \frac{1+2s^2t^2-t^2}{st(1+t^2)}\sin ksd \sin ktd & -s\sin ksd - \frac{1}{t}\sin ktd & \cos ksd - \cos ktd \\
\frac{3-t^2}{1+t^2}(1-\cos ksd \sin ktd) + \frac{1+2s^2t^2-t^2}{st(1+t^2)}\sin ksd \sin ktd & \frac{1}{s}\sin ksd \cos ktd + t\cos ksd \sin ktd & -\cos ksd + \cos ktd & -\frac{1}{s}\sin ksd - t\sin ktd \\
-s\sin ksd - \frac{1}{t}\sin ktd & -\cos ksd + \cos ktd & \frac{1}{t}\cos ksd \sin ktd + s\sin ksd \cos ktd & \frac{t^2-3}{1+t^2}(1-\cos ksd \cos ktd) + \frac{t^2-2s^2t^2-1}{st(1+t^2)}\sin ksd \sin ktd \\
\cos ksd - \cos ktd & -\frac{1}{s}\sin ksd - t\sin ktd & \frac{t^2-3}{1+t^2}(1-\cos ksd \cos ktd) + \frac{t^2-2s^2t^2-1}{st(1+t^2)}\sin ksd \sin ktd & \frac{1}{s}\sin ksd \cos ktd + t\cos ksd \sin ktd
\end{bmatrix}
\begin{Bmatrix} u_1 \\ w_1 \\ u_2 \\ w_2 \end{Bmatrix}
$$

$$D = 2(1-\cos ksd \cos ktd) + (st + \frac{1}{st})\sin ksd \sin ktd\,, \qquad s = -i\sqrt{1-\frac{\omega^2}{(V_p^* k)^2}}\,, \qquad t = -i\sqrt{1-\frac{\omega^2}{(V_s^* k)^2}}$$

The interest in this analysis was for an axisymmetric case of oscillations of a circular plate on the surface of a layered system. Therefore only the in-plane motion was considered. Satisfying the radiation condition of no incoming waves the stiffness matrix of the half-space can be derived from the stiffness matrix of a layer as shown in Table II.

Table II. The stiffness matrix of a half-space.

$$
\begin{Bmatrix} P_0 \\ R_0 \end{Bmatrix} = kG^*
\begin{bmatrix}
\frac{is(1+t^2)}{1+st} & 2-\frac{1+t^2}{1+st} \\
2-\frac{1+t^2}{1+st} & \frac{it(1+t^2)}{1+st}
\end{bmatrix}
\begin{Bmatrix} u_0 \\ w_0 \end{Bmatrix}
$$

Using principles analogous to the Finite Element Method the system stiffness matrix of a layered system can be assembled to the form

$$\mathbf{S}\ \mathbf{u} = \mathbf{p} \tag{3}$$

where **p** represents the vector of external loading at layer interfaces, **u** the displacement vector and **S** the system stiffness matrix.

Again, since Rayleigh modes represent natural modes of oscillations of the medium, they can be defined as a solution of an eigenvalue problem

$$\mathbf{S}(\omega, k)\,\mathbf{u} = \mathbf{0} \tag{4}$$

where for a fixed angular frequency ω an eigenvalue ωk represents a phase velocity of a Rayleigh wave while **u** represents its shape as a function of depth. Because the elements of the stiffness matrix are transcendental functions, theoretically an infinite number of modes are possible.

In a case of an external harmonic loading at layer interfaces, the loading needs first to be transformed from the spatial domain to the frequency-wave number domain. It is done in terms of Fourier transforms for Cartesian coordinates and in terms of Fourier series in the circumferential direction and Hankel transforms in the radial direction for cylindrical coordinates. Then the corresponding displacements in the frequency-wave number domain can be obtained according to Eq. 3.

For an assumed uniform vertical circular loading q with a radius R at the surface of a layered system, the vertical displacement at the surface at the distance r from the center of the loading can be expressed as

$$w(r) = qR\int_0^\infty J_1(kR)\,J_0(kr)\,w_0(k)\,dk \tag{5}$$

where $w_0(k)$ is the vertical surface displacement in the frequency-wave number domain due to unit loading q and J_0 and J_1 Bessel functions of the first kind of the order zero and one, respectively.

The rate of energy transmission in the horizontal direction E_r is defined as

$$E_r = -\frac{1}{2}\int_0^d \big(Re[\sigma_x(z)]\,Re[\dot{u}(z)] + Im[\sigma_x(z)]\,Im[\dot{u}(z)] + Re[\tau_{xz}(z)]\,Re[\dot{w}(z)] + Im[\tau_{xz}(z)]\,Im[\dot{w}(z)]\big)\,dz \tag{6}$$

and represents the amount of energy propagating over the depth d of a layer and averaged over a period $2\Pi/\omega$. For the purpose of evaluating the contribution of the i^{th} layer with respect to the total rate of energy transmission the normalized rate is defined as

$$E_{rni} = \frac{E_{ri}}{\sum_{j=1}^{n} E_{rj}} \tag{7}$$

where n is the total number of layers, including the half-space.

NUMERICAL RESULTS

Results of an extensive study of the influence of the soil stratification on the participation of higher Rayleigh modes in the overall wave propagation is presented for a two-layer over a half-space system. The results include the dispersion curves of several lowest Rayleigh modes, modal shapes and the normalized rate of energy transmission. They also include vertical surface displacements in the frequency-wave number and the spatial domain due to harmonic vertical circular loading at the surface of a layered system. The following dimensionless parameters are defined and used in interpretation of input variables and results:

- shear wave velocity ratio $\underline{V}_{sj}=V_{sj}/V_{s1}$,
- mass density ratio $\underline{\rho}_j=\rho_j/\rho_1$,
- thickness ratio $\underline{d}_j=d_j/d_1$,
- dimensionless wavelength $\lambda_0=\lambda_{ph}/d_1$,
- dimensionless frequency $\omega_0=\omega d_1/V_{s1}$, and
- dimensionless frequency $a_0=\omega R/V_{s1}$,

where the subscript j indicate properties of a layer j, the subscript 1 properties of the top layer, and the subscript ph values related to a phase velocity of a Rayleigh wave. Since the dimensionless parameters loose their advantage in simple interpretation of results for systems with two or more layers, the following figures are described also in terms of actual physical properties used in calculations. For the purpose of this study Poisson's ratio ν and the damping ratio ξ were held constant for all layers and the half-space as 0.35 and 0.05%, respectively.

Two two-layer over a half-space systems are compared in terms of elements defined in the preceding section. The systems have the thickness and the mass density ratio equal to 1, while the shear wave velocity ratios for system 1 are $\underline{V}_{s2}$=1.33 and $\underline{V}_{s3}$=1.67, and for system 2, $\underline{V}_{s2}$=0.75 and $\underline{V}_{s3}$=1.2 . Figure 7 represents the dispersion curves for the first several modes for both systems. System 1 exhibits stronger separation of the modes than system 2, especially for frequencies above 25 Hz, or in terms of the dimensionless frequency ω_0, for system 2 above 2. The corresponding wavelengths are less than 30 ft, or in terms of the dimensionless wavelength λ_0 less than 1.5 . The same dispersion curves are presented later in Figs. 13 and 14 in the wavelength-phase velocity relationship. Cut-off frequencies of higher Rayleigh modes where the phase velocity reaches the shear wave velocity of the half-space can also be observed.

Response of systems subjected to a harmonic vertical circular at their surface can be obtained in the frequency-wave number according to Eq. 3, and in the spatial domain according to Eq. 5. The series of plots in Fig. 8 shows the vertical surface displacements for both systems in the frequency-wave number domain for the range of frequencies from 5 to 60 Hz. The figure clearly indicates that while in system 1 the first mode maintains a dominant role through the entire frequency range, in system 2 the dominant role is transferred from the first toward higher modes as frequency increases. It is significant to observe that the frequency at which the domination is transferred from the first to the second mode matches very well the localized approach of dispersion curves of corresponding dispersion curves in Fig. 7. Similarly, the frequency at which the domination is further transferred to the third mode matches well the approach of the dispersion curves of the second and the third mode.

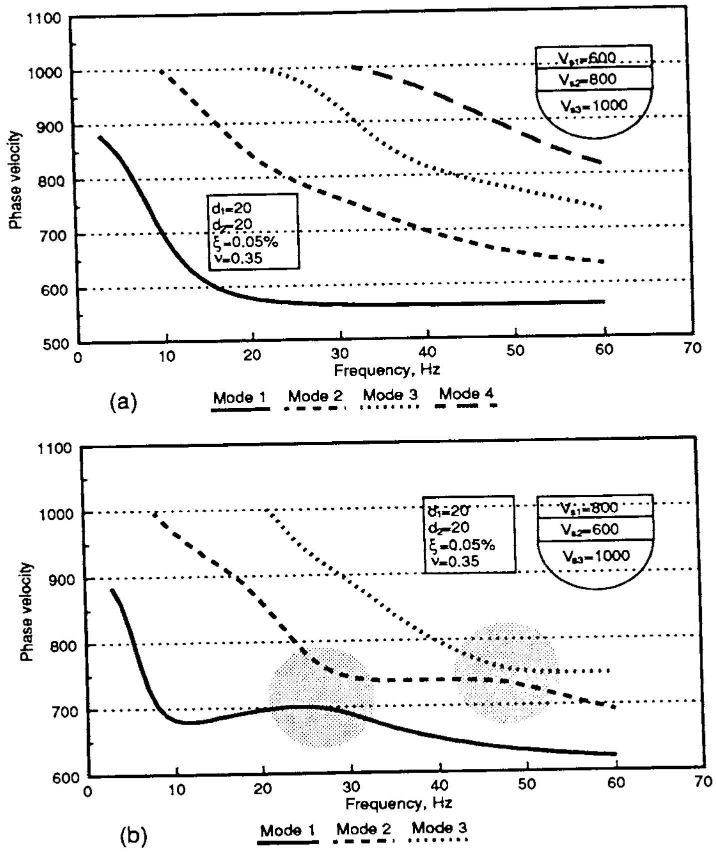

Fig. 7. Dispersion curves for two-layer over a half-space systems. (a) $\underline{V}_{s2}$=1.33 and $\underline{V}_{s3}$=1.67, (b) $\underline{V}_{s2}$=0.75 and $\underline{V}_{s3}$=1.2 .

The analysis of the normalized rate of energy transmission, as defined by Eqs. 6 and 7, indicates that in system 1 a dominant part of energy for all modes is concentrated in the area close to the surface, except for a narrow range of low frequencies. This is illustrated in Fig. 9a for the first mode. In contrast to system 1, system 2 exhibits very irregular behavior with an exchange of concentration of energy transmission between layers as shown in Fig. 9b for the first mode. Again it can be observed from Fig. 9b that the frequency at which the dominant portion of energy of the first mode switches from the first to the second layer, and for the second mode from the second to the first layer matches the approach of the dispersion curves of corresponding modes in Fig. 7b. The same observation is valid for the exchange of the rates of energy transmission between layers for the second and the third mode.

Probably the most important observation is that the transition of energy transmission towards the top layer for all modes occurs at about the natural frequency of the corresponding modes for the top layer fixed at its base. The natural frequencies expressed by the dimensionless frequency ω_0 are $\Pi/2$, $3\Pi/2$, $5\Pi/2$ etc., which for system 1 correspond to 10, 30, 50...Hz.

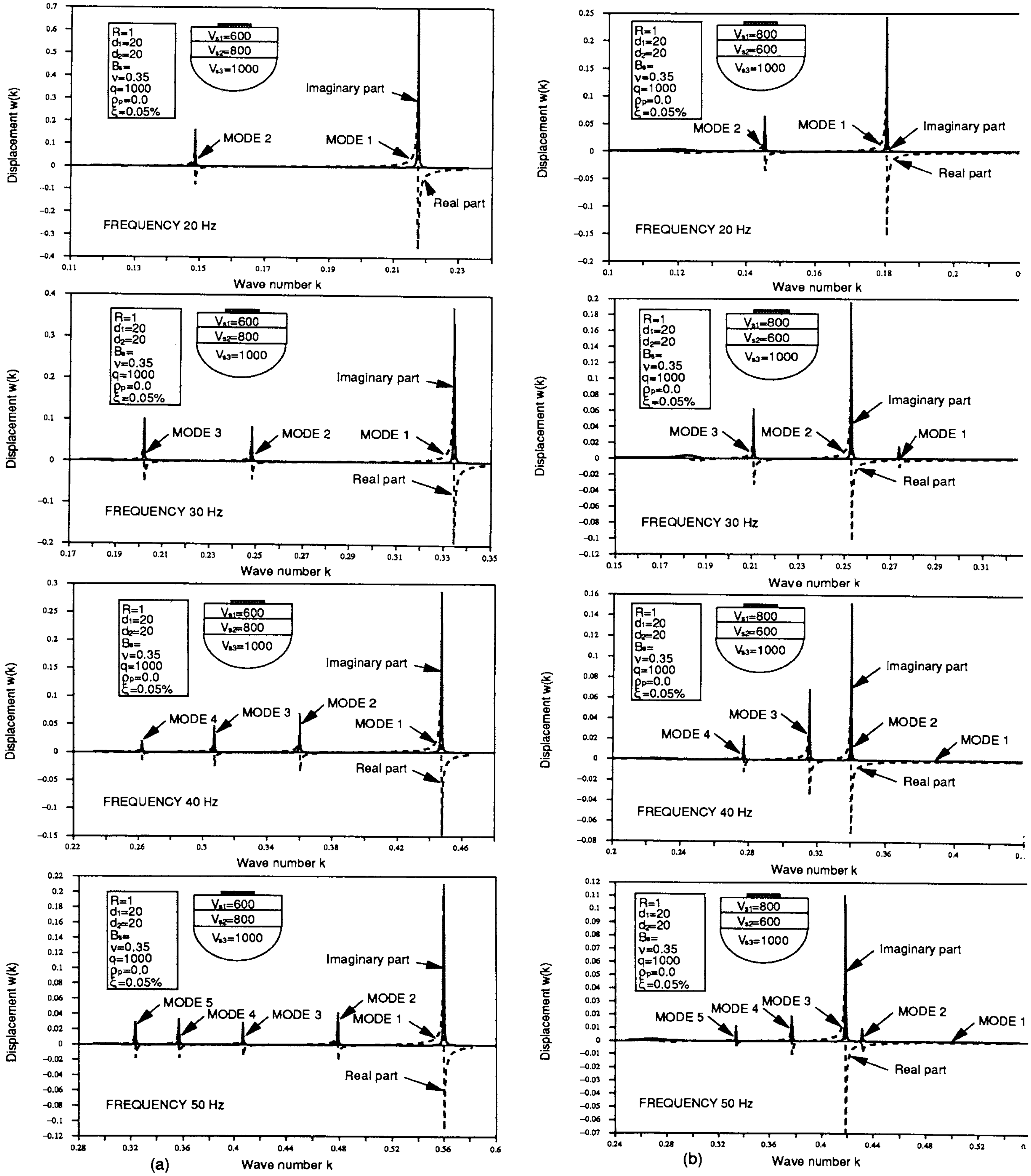

Fig. 8. Vertical surface displacements due to a vertical harmonic circular loading in the frequency-wave number domain. (a) $\underline{V}_{s2}$=1.33, $\underline{V}_{s3}$=1.67, (b) $\underline{V}_{s2}$=0.75, $\underline{V}_{s3}$=1.2 .

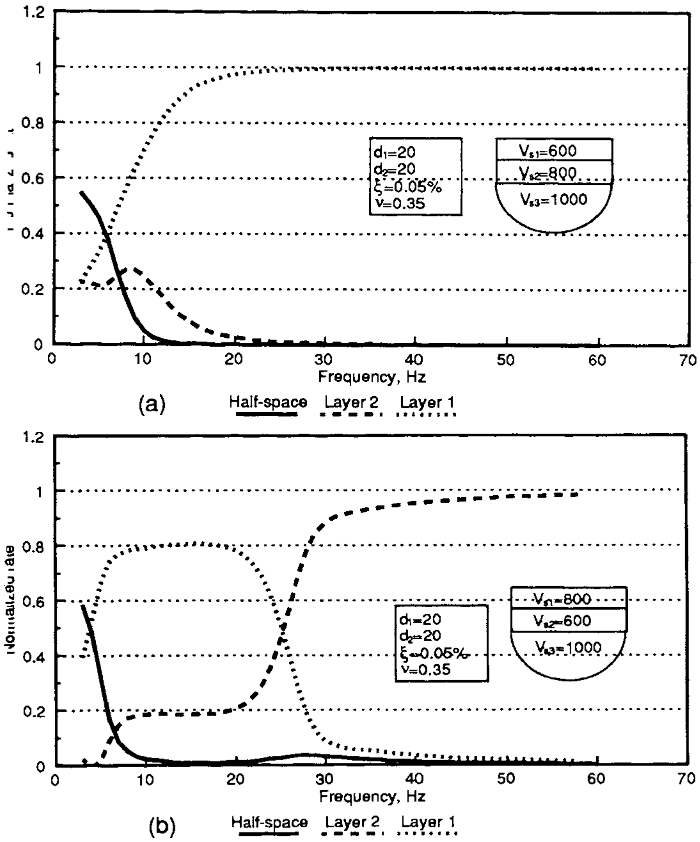

Fig. 9. The normalized rate of energy transmission for the first Rayleigh mode. (a) $\underline{V}_{s2}$=1.33, $\underline{V}_{s3}$=1.67, (b) $\underline{V}_{s2}$=0.75, $\underline{V}_{s3}$=1.2 .

The vertical surface displacements of several lowest Rayleigh modes due to the same harmonic circular loading are shown in Fig. 10. The displacements were calculated at approximately two Rayleigh wave wavelengths from the source. It was done at that distance because the displacements calculated in the spatial coordinates have shown that well developed propagating waves start there. As an additional confirmation to the previous observations is that system 1 keeps the dominant influence of the first mode, while system 2 transfers the influence from the first towards higher modes at frequencies which match closely approaches of dispersion curves.

The comparison of shapes of the vertical component of the displacement of Rayleigh modes in Fig. 11 indicates that for system 1 the shapes are preserved with a frequency increase. The modal shapes correspond well to the shapes of natural oscillations of a cantilever shear beam. A decrease in depth of penetration of the body as frequency increases represents the only major change. A dominant portion of the first mode is concentrated near the surface and its shape is very similar to the shape of a Rayleigh wave in a half-space. For system 2, major changes can be noticed with frequency increase. The shape closest to the shape of a Rayleigh wave in a half-space has the first mode at 20 Hz, the second mode at 40 Hz, and the third mode at 60 Hz. Also, the transfer of the major portion of the wave from the first to the second layer and opposite confirms the observations on the transfer of the rate of energy transmission. Even though mode shapes of the horizontal component of a Rayleigh wave were not discussed and presented, the results show behavior analogous to the vertical component.

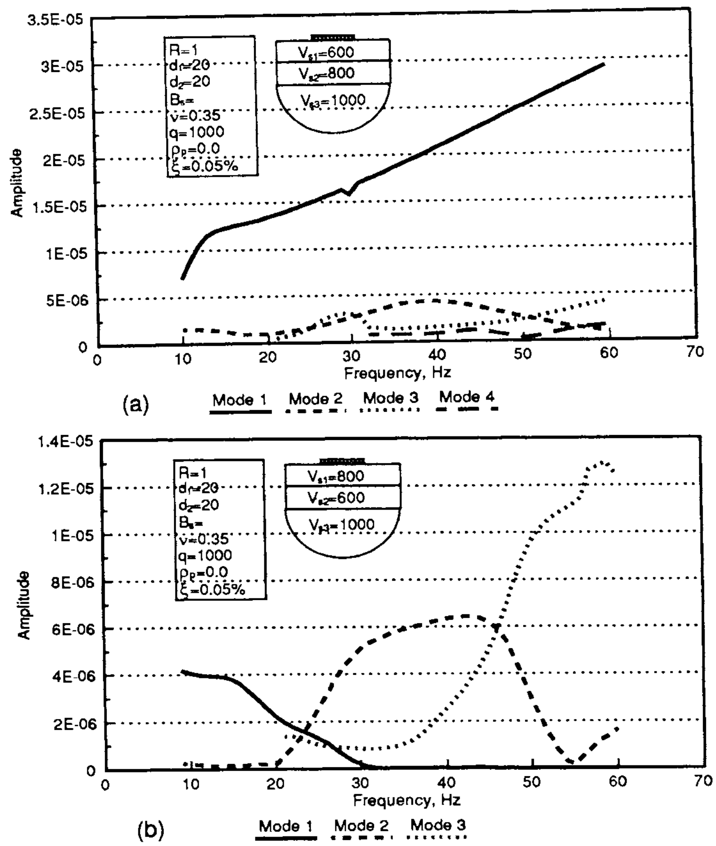

Fig. 10. Surface vertical displacements at the distance $r=2V_{s1}/f$ of several Rayleigh modes due to uniform harmonic circular loading. (a) $\underline{V}_{s2}$=1.33, $\underline{V}_{s3}$=1.67, (b) $\underline{V}_{s2}$=0.75, $\underline{V}_{s3}$=1.2 .

Finally, the circular harmonic source of vibrations was numerically simulated so that vertical surface displacements in the spatial coordinates were evaluated according to Eq. 5. It was actually a simulation of the SASW measurement for a particular frequency. The difference exists in the fact that the impact source in the SASW measurement is generally some kind of a hammer which can be considered more or less as a rigid plate, while the uniform loading can be viewed as an infinitely flexible plate with uniform loading. For low values of the dimensionless frequency a_0, the rigidity of the plate is of no practical importance.

The principal goal of this part of the analysis was to develop displacement curves for a set of frequencies, evaluate wavelengths of dominant waves and based on them construct the "simulated" dispersion curves. The example of the displacement curve for system 2 at 40 Hz is shown in Fig. 12. The wavelength is measured as shown in the figure, but evaluated as an average of two to three cycles of both the real and the imaginary component. Because a portion of the wave close to the source, approximately 1 to 2 wavelengths, has more characteristics of a standing than a propagating wave, and because there are significant variations in the wavelength of that portion, it was not considered in the evaluation. The dispersion curves evaluated in this way for systems 1 and 2 are presented together with theoretically defined dispersion curves for several Rayleigh modes in Figs. 13 and 14.

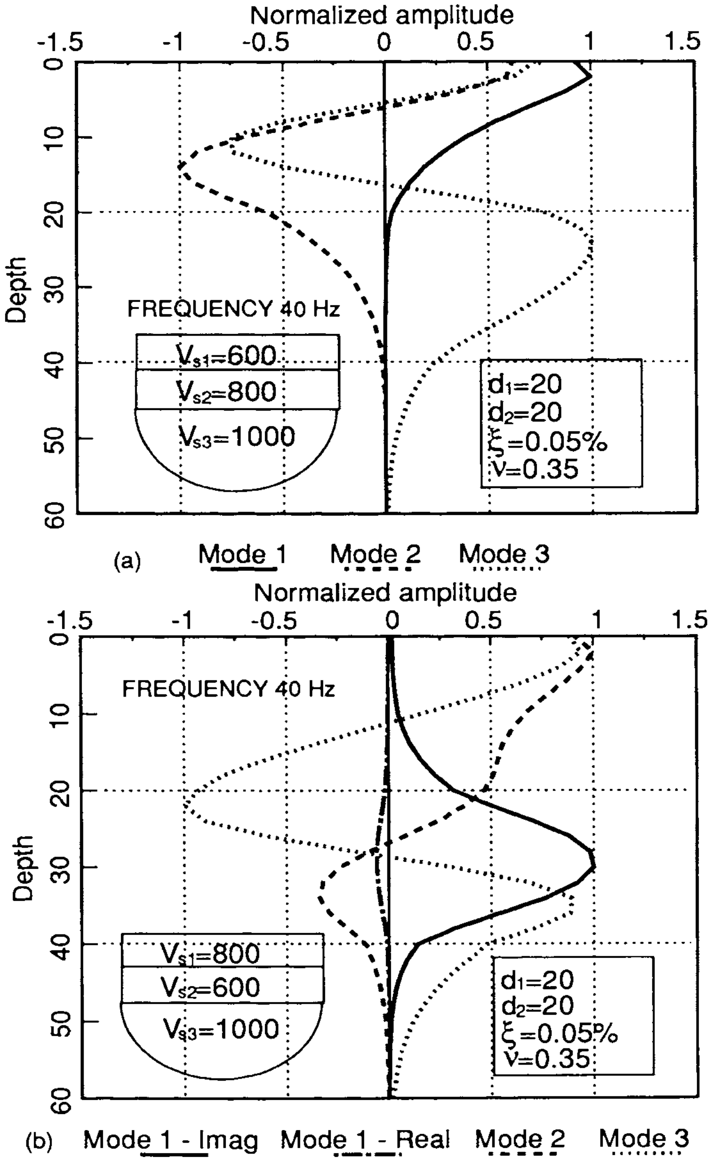

Fig. 11. Shapes of the vertical component of the first three modes. (a) $\underline{V}_{s2}$=1.33, $\underline{V}_{s3}$=1.67, (b) $\underline{V}_{s2}$=0.75, $\underline{V}_{s3}$=1.2 .

Figure 13 represents the dispersion curves for system 1. It can be observed that in both the frequency-phase velocity and wavelength-phase velocity presentation the "simulated" dispersion curve follows very well the dispersion curve of the first Rayleigh mode. The "simulated" curve

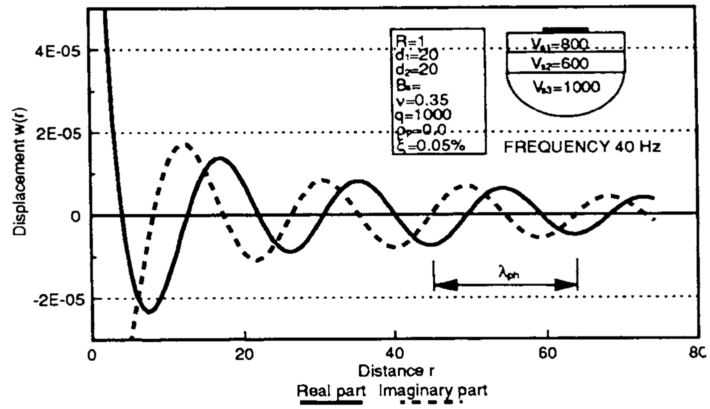

Fig. 12. Surface vertical displacement due to uniform harmonic circular loading for system 2 with $\underline{V}_{s2}$=0.75 and $\underline{V}_{s3}$=1.25.

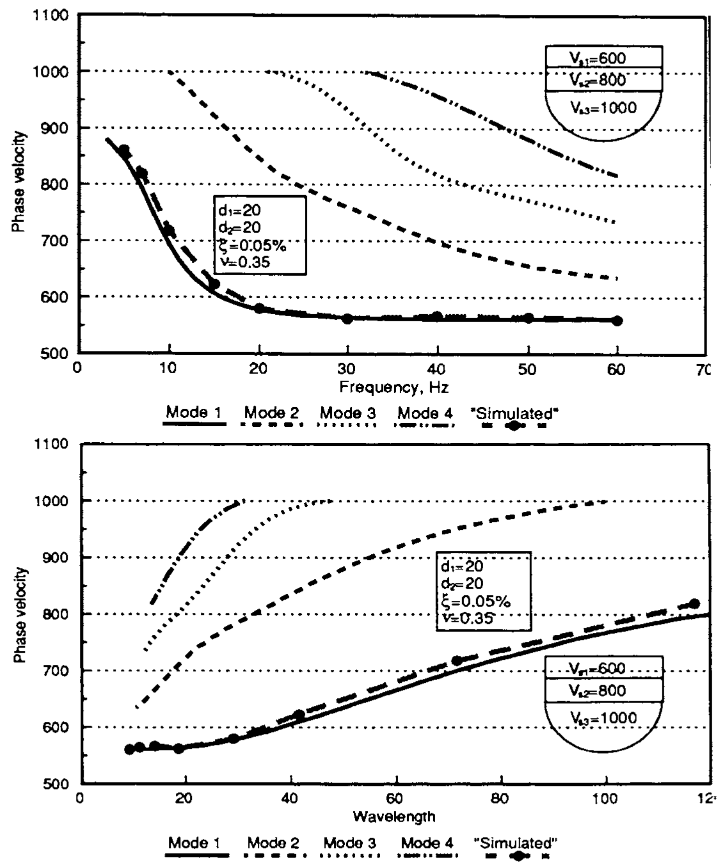

Fig. 13. Theoretical dispersion curves for the first four Rayleigh modes and the "simulated" dispersion curve for system 1 with $\underline{V}_{s2}$=1.33 and $\underline{V}_{s3}$=1.67 . (a) frequency-phase velocity relationship, (b) wavelength-phase velocity relationship.

of system 2 represented in the Fig. 14a in the frequency-phase velocity relationship confirms all the previous observations on the frequency of transition of influence from one to another mode. The transition zone is characterized by a localized approach of dispersion curves of two modes. The presentation in the wavelength-phase velocity relationship indicates that the transition zones match very well sudden changes in curvatures of the dispersion curves, as the approaches between dispersion curves. Because dispersion curves during the inversion process of the SASW test are presented usually in the wavelength-phase velocity relationship form this observation is of a special importance.

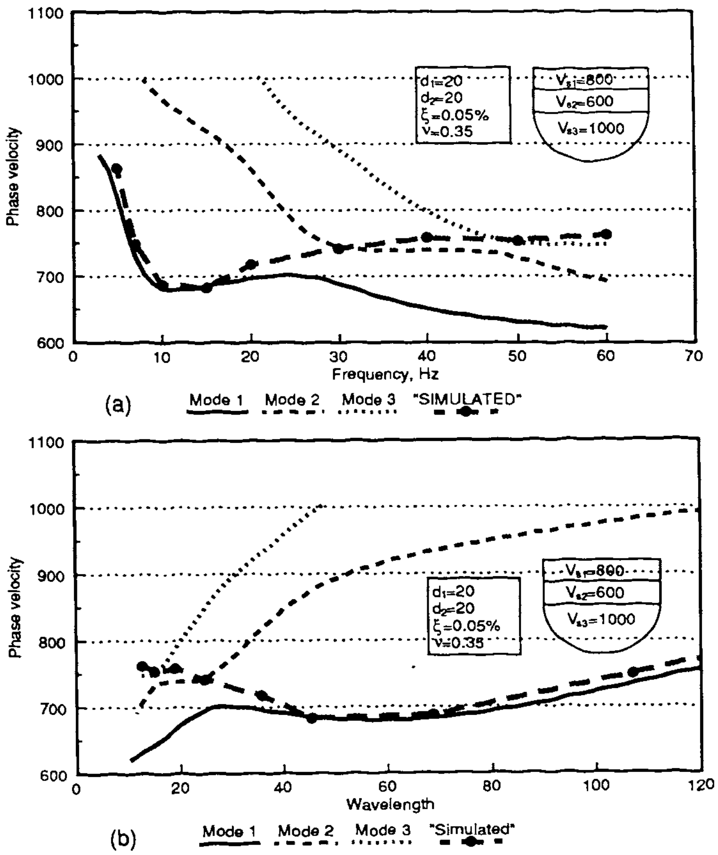

Fig. 14. Theoretical dispersion curves of the first three Rayleigh modes and the "simulated" dispersion curve for system 2 with V_{s2}=0.75 and V_{s3}=1.25 . (a) frequency-phase velocity relationship, (b) wavelength-phase velocity relationship.

As an additional example of the transition of influence between Rayleigh modes a two-layer over a half-space system with sharper contrasts in layer properties than system 2 is presented. The shear wave velocity ratios in this case were V_{s2}=0.6 and V_{s3}=1.2 . The obtained dispersion curves and the vertical surface displacements shown in Figs. 15 and 16 confirm observations stated in the previous paragraphs for system 2.

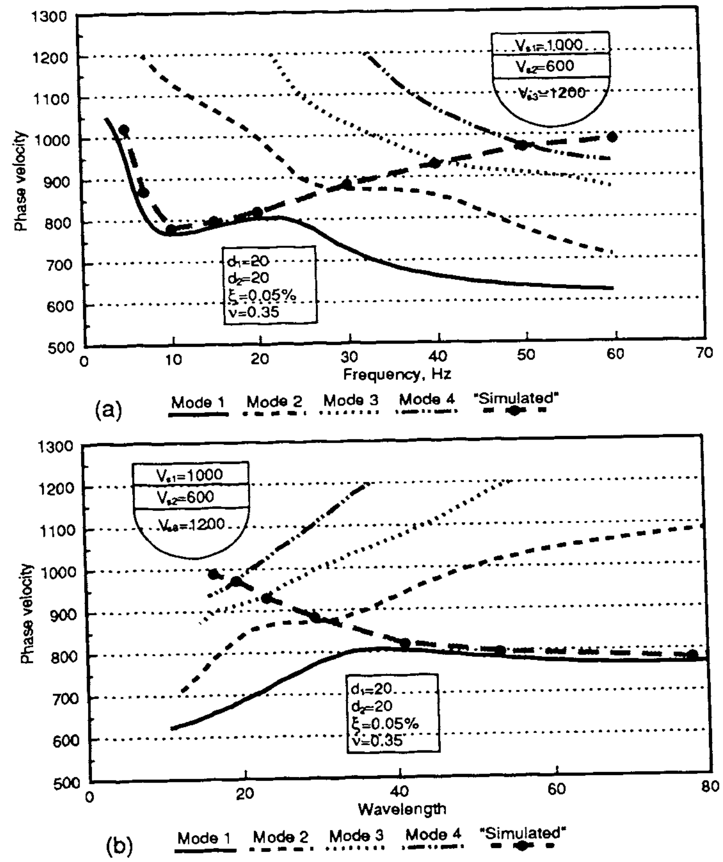

Fig. 15. Theoretical dispersion curves of the first four Rayleigh modes and the "simulated" dispersion curve for the system with V_{s2}=0.6 and V_{s3}=1.2 . (a) frequency-phase velocity relationship, (b) wavelength-phase velocity relationship.

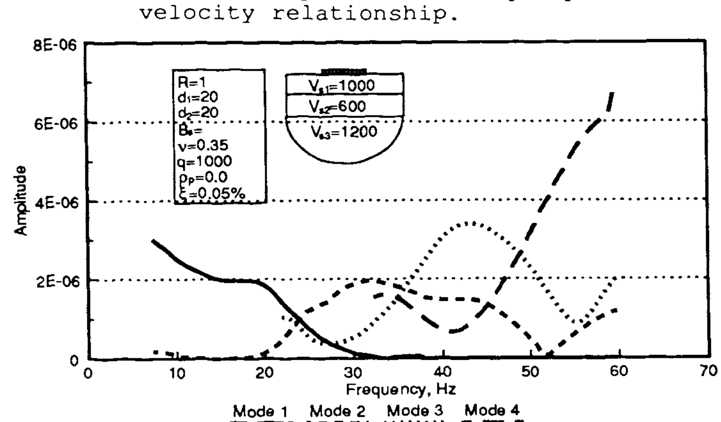

Fig. 16. Vertical surface displacements at the distance $r=2V_{s1}/f$ of several Rayleigh modes due to uniform harmonic circular loading for the system with V_{s2}=0.6 and V_{s3}=1.2 .

CONCLUSIONS AND RECOMMENDATIONS

1. For the purpose of SASW testing a study of the influence of soil stratification on the level of participation of higher Rayleigh modes in surface wave propagation was conducted. The study included generation and the analysis of dispersion curves and mode shapes for multiple Rayleigh modes, and the analysis of the wave propagation due to harmonic vertical circular loading at the surface of a layered system. The later analysis included evaluation of "simulated" dispersion curves, the normalized rate of energy transmission, vertical surface

displacements in the frequency-wave number and the spatial domain, and modal vertical surface displacements.

2. All the results of the analysis of profiles at which the shear wave velocity of layer increases with depth indicate that the first Rayleigh mode stays dominant through the entire frequency range. The dispersion curves are well separated, shapes of the vertical component of modes correspond well to natural forms of oscillations of a cantilever shear type structure, concentration of energy transmission occurs for all modes near the surface, except for a narrow range of low frequencies. Therefore, a field evaluated dispersion curve, like a "simulated", matches well the dispersion curve of the theoretical first Rayleigh mode.

3. The results of the analysis on profiles at which the shear wave velocity has an irregular pattern with depth indicate that higher Rayleigh modes can have a dominant role in wave propagation along the surface of a layered medium. Since the variation of cases which could be analyzed is so broad, the following conclusions are related only to the results of the analysis of a two-layer over the half-space systems where a softer layer exists between a stiffer surface layer and the half-space.
(a) The dispersion curves contain localized approaches which represent the transition of domination from one mode to another. The "simulated" dispersion curve crosses the dispersion curve of any particular mode in the neighborhood of the natural frequency of the corresponding mode of the top layer over a rigid base.
(b) The shape of the dominant Rayleigh mode is close to the shape of the Rayleigh wave in the half-space.
(c) The transmission of energy of the dominant mode is concentrated near the surface, while for the other modes it may occur deeper. This is closely related to the conclusion b.

Above conclusions indicate that the portions of a field evaluated dispersion curve of a profile with an irregular pattern can strongly be affected by higher Rayleigh modes. Therefore, the inversion process should not be guided by the theoretically defined first mode only. The simplest element in the identification of a potential significant contribution of higher modes is the observation of approaches of dispersion curves between two modes.

4. The following are recommendations for future research:
(a) To obtain more general conclusions on the participation of higher Rayleigh modes in the wave propagation along the surface of soil systems a more extensive parametric study is needed.
(b) To improve the inversion process of the SASW testing procedure, an algorithm is needed which would in addition to the definition of theoretical dispersion curves include the evaluation of the contribution of each of the modes to the overall solution. It can be done by analyzing mode shapes, the rate of energy transmission or by actual numerical simulation of wave propagation due to a circular impact source. The latest would lead to the inversion process in which the field and the "simulated" dispersion curve would be compared only.

REFERENCES

Douglas, R.A. and Eller, G.L. (1986), "Nondestructive Pavement Testing by Wave Propagation: Advanced Methods of Analysis and Parameter Management", Transportation Research Record No. 1070, 53-62.

Ewing, W.M., Jardetzky, W.S. and Press, F. (1957), Elastic Waves in Layered Media, McGraw-Hill Book Company, Inc., New York, NY.

Haskell, N.A. (1953), "The Dispersion of Surfac Waves in Multilayered Media", Bulletin of Seismological Society of America, Vol.43, No. 1, 17-43.

Hiltunen, D.R. and Woods, R.D. (1988), "SASW an Crosshole Test Results Compared", Earthquak Engineering and Soil Dynamics II - Recent Advances in Ground-Motion Evaluation, Proceedings of the Specialty Conference of Geotechnical Engineering Division at Park City, Utah, ASCE, New York, NY, 279-289.

Kausel, E. and Roesset, J.M. (1981), "Stiffness Matrices for Layered Soils", Bulletin of Seismological Society of America, Vol. 71, No. 6, 1743-1761.

Nazarian, S., Stokoe, K.H. II and Hudson, W.R. (1983), "Use of Spectral Analysis of Surface Waves Method for Determination of Moduli and Thicknesses of Pavement Systems", Transportation Research Record, No. 930, 38-45.

Nazarian, S. (1984), In Situ Determination of Elastic Moduli of Soil Deposits and Pavement Systems by Spectral-Analysis-of-Surface-Waves Method, Ph.D. Dissertation, Civil Engineering Department, University of Texas at Austin.

Nazarian, S. and Stokoe, K.H. II (1984), "Nondestructive Testing of Pavements Using Surface Waves", Transportation Research Record, No. 993, 67-79.

Nazarian, S. and Stokoe, K.H. II (1986) , "Use of Surface Waves in Pavement Evaluation", Transportation Research Record, No. 1070, 132-144.

Sanchez-Salinero, I., Roesset, J.M., Shao, K.-Y., Stokoe, K.H. II and Rix, G.J. (1987), "Analytical Evaluation of Variables Affecting Surface Wave Testing of Pavements", Transportation Research Record, No. 1136, 86-95.

Thomson, W.T. (1950), "Transmission of Elastic Waves Through a Stratified Soil Medium", Journal of Applied Physics, Vol.21, 89-93.

Wolf, J.P. and Obernhuber, P. (1982), "Free-Field Response from Inclined SV- and P-Waves and Rayleigh-Waves", Earthquake Engineering and Structural Dynamics, Vol. 10, 847-869.

Wolf, J.P. (1985), Dynamic Soil-Structure Interaction, Prentice-Hall, Inc., Englewood Cliffs, NJ.